Computer Assisted Mechanics and Engineering Sciences, 9: 359–371, 2002.

Dynamics of a sprayer with large flexible boom[1]

Marian Gofron
Technology Center, Case Corporation
7 South 600 County Line Road, Burr Ridge, IL 60521, USA

(Received August 8, 2000)

The quality of spraying chemicals in a field depends on the distance between the boom of the sprayer and the canopy. Keeping that distance relatively constant enables even distribution of chemicals over the field. However, because the boom has a significant moment of inertia due to its length, (commonly 30 [m] and above) the vehicle has a tendency to roll. The excessive rolling significantly decreases the quality of spraying and can even cause damage to the boom if the tip of the boom hits the ground. The boom itself deflects significantly due to its flexibility and can increase the total amplitude of the boom tip point movement during spraying operation. In this study the effect of the boom flexibility on vehicle rolling, boom rolling and boom reaction forces is evaluated. Also the effect of number of modes selected to represent flexible model, on the boom tip point deflection is analyzed. The simulation model of the sprayer is developed in DADS multibody code and mode shapes of the boom are obtained from I-DEAS code. The simulation model of the sprayer is driven over a ramp and a numerical representation of the NATC (Nevada Automotive Test Center) track.

1. Introduction

Perfect spraying would distribute the same amount of chemicals per unit area throughout the entire field. Local under-application may not remove weeds entirely from the area or eventual over-application may have a negative impact on the environment. The actual spraying quality depends entirely on sprayer performance in the field. Some sprayers, due to their superior suspension and boom design, distribute chemicals more evenly than others do. From the spraying quality point of view, the critical elements of a sprayer design are its suspension, possible boom suspension, and flexibility of the boom itself. It is desired that the boom would maintain a constant distance from the field canopy, and move steadily over the entire field length. Vertical and rolling boom motions cause changes in the overlap of the spray cones of the individual nozzles. Additionally, eventual fore and aft movement of the boom, due to its flexibility in the horizontal direction, imparts a fluctuating deposit of spray liquid in the driving direction and thus further reducing quality of the chemical distribution.

A significant amount of research is currently being done in order to evaluate existing sprayers and to develop new sprayers with superior chemical distribution. Chaplin and Wu [1] developed a computer model that predicts the motion of a sprayer boom in two dimensions. The model has been verified in the laboratory by dropping one wheel of the sprayer and observing the boom displacement for various tire pressures and water volumes in the sprayer tank. The motion of the water in the sprayer tank, represented by a pendulum, was incorporated into the model to represent the sloshing of the water in the sprayer tank. It has been found that over 40% improvement in the predicted evenness of spray distribution was achieved by reducing the tank water volume from nearly full to nearly empty. The authors also found that other factors such as tank shape and orientation, boom suspension, boom location, tire-axle configuration, and surface profile, may have an effect on the boom motion.

[1]This is an extended version of the article presented at the NATO Advanced Research Workshop on the *Computational Aspects of Nonlinear Structural Systems with Large Rigid Body Motion*, Pułtusk, Poland, July 2–7, 2000.

To develop an inexpensive test method to evaluate field sprayers [10, 12], Sinfort et al. [12] proposed a simulation method based on a track simulator which can reproduce pre-recorded tracks, standard tracks or any movement programmed by the user. Movements of the boom are measured with an infrared sensor and used to calculate spray distribution. Initially in the project, field tests were set-up and later reproduced with the simulation method. Simulated results were compared with distribution results measured during actual field tests. The main objective in the development of new generation sprayers is to stabilize the boom. One of the ideas is to use an active boom suspension system [11]. The comparison between well performing passive system and the active system has been done by Nielsen and Sorensen. They simulated both systems on a constructed surface and found that the active system performs much better than the passive. The boom followed the signals almost perfectly, and the energy consumption was less than 15 watts.

One of the techniques to model flexibility of a boom is to use a modal model of a boom. Langenakens et al. [7, 8, 9] obtained the modal model of the boom by measuring accelerations at different points on the structure and calculating Frequency Response Functions. These techniques are used to formulate the equations of motion of a tractor equipped with a spray installation. This numerical model is later used to calculate forced responses to stochastic disturbances representing the tractor driving over rough fields. Using their model the authors analyzed the effect of rigid body motions, flexible deformation of the sprayer boom, driving speed [9] and tire pressure on spray distribution. Based on their analysis, it has been concluded that the vertical [7] and horizontal [8] boom movements generated by vehicle bouncing, pitching, and rolling, as well as flexible motion of the sprayer, have a large effect on the spray distribution and should be avoided. It has also been shown that the tire pressure has smaller influence on the spray distribution than the forward speed of the vehicle. The tire pressure had little effect on the boom vibrations. However, a small increase in boom movement caused a disproportional degradation in the spray distribution. As a result of the simulations, the authors concluded that a more homogeneous deposition of chemicals could be obtained at lower forward velocities and minimal tire pressure.

Another alternative to model flexibility of the boom is to use the finite element approach [5, 6]. Kennes et al. [6] validated a finite element model of the boom. The power spectra density of measured and modeled velocity of the boom tip matched very closely. Their conclusion opens possibilities to investigate the effect of structural adaptations to existing sprayers without the need for time-consuming prototyping. Another advantage is that the simulated boom movements can be used as input to calculate spray pattern on the soil. In [5], the authors developed and analyzed a prototype passive horizontal suspension system. Different boom suspension set-ups were compared with regard to boom vibrations and spray pattern homogeneity. As in [6] the boom is modeled using the finite element approach. Based on the analysis, the authors concluded that an appropriate passive suspension is able to decrease the coefficient of variance of spray deposition by almost 50%.

In this study a finite element model of the boom has been developed and used to obtain modal characteristics of the structure. These characteristics have been incorporated into a multibody model of the sprayer that had been validated with the real vehicle in the earlier studies. The effect of selected number of modes on the boom deformation and the effect of flexibility on boom reaction forces and vehicle and boom rolling have been analyzed. This approach, based on computer modeling of the sprayer together with various field conditions, can be used to quickly evaluate various boom designs and vehicle and boom suspension concepts.

2. Multibody representation of a sprayer

In this investigation, a sprayer multibody model that consists of interconnected rigid and deformable bodies is analyzed using the augmented formulation in which the constraint equations that describe mechanical joints and specified motion trajectories are adjoined to the system differential equations using the vector of Lagrange multipliers [3, 4, 5]. The kinematic constraint equations can be written

in a vector form as

$$\mathbf{C}(\mathbf{q}, t) = 0 \tag{1}$$

where $\mathbf{C}(\mathbf{q}, t) = [\, C_1(\mathbf{q}, t) \;\; C_2(\mathbf{q}, t) \;\; \ldots \;\; C_{n_c}(\mathbf{q}, t) \,]^T$ is the vector of algebraic holonomic constraint equations, n_c is the total number of constraints, $\mathbf{q}$ is the total vector of system generalized coordinates, and t is time. Using the technique of Lagrange multipliers, the dynamic differential equations of motion of the constrained flexible mechanical system can be written as

$$\mathbf{M}\,\ddot{\mathbf{q}} + \mathbf{C}_\mathbf{q}^T \boldsymbol{\lambda} = \mathbf{Q}_e + \mathbf{Q}_v \tag{2}$$

where $\mathbf{M}$ is the system mass matrix, $\mathbf{C}_\mathbf{q}$ is the Jacobian matrix of the kinematic constraints, $\boldsymbol{\lambda}$ is the vector of Lagrange multipliers, $\mathbf{Q}_e$ is the vector of externally applied and elastic forces, and $\mathbf{Q}_v$ is the vector of Coriolis and centrifugal forces. The vector of system generalized coordinates can be written as

$$\mathbf{q} = [\, \mathbf{q}_r^T \;\; \mathbf{q}_f^T \,]^T \tag{3}$$

where $\mathbf{q}_r$ is the vector of reference coordinates, and $\mathbf{q}_f$ is the vector of elastic coordinates. According to the generalized coordinate partitioning of Eq. (3), Eq. (2) can be written in a partitioned matrix form as

$$\begin{bmatrix} \mathbf{M}_{rr} & \mathbf{M}_{rf} \\ \mathbf{M}_{fr} & \mathbf{M}_{ff} \end{bmatrix} \begin{bmatrix} \ddot{\mathbf{q}}_r \\ \ddot{\mathbf{q}}_f \end{bmatrix} + \begin{bmatrix} \mathbf{C}_{\mathbf{q}_r}^T \\ \mathbf{C}_{\mathbf{q}_f}^T \end{bmatrix} \boldsymbol{\lambda} = \begin{bmatrix} (\mathbf{Q}_e)_r \\ (\mathbf{Q}_e)_f \end{bmatrix} + \begin{bmatrix} (\mathbf{Q}_v)_r \\ (\mathbf{Q}_v)_f \end{bmatrix} \tag{4}$$

where subscripts r and f refer, respectively, to reference and elastic coordinates. Differentiating the constraints of Eq. (1) twice with respect to time one obtains

$$\mathbf{C}_\mathbf{q}\,\ddot{\mathbf{q}} = \mathbf{Q}_c \tag{5}$$

where $\mathbf{Q}_c$ is a vector that absorbs terms that are quadratic in the velocities. Note that Eq. (5) can be written as

$$[\, \mathbf{C}_{\mathbf{q}_r} \;\; \mathbf{C}_{\mathbf{q}_f} \,] \begin{bmatrix} \ddot{\mathbf{q}}_r \\ \ddot{\mathbf{q}}_f \end{bmatrix} = \mathbf{Q}_c \,. \tag{6}$$

Combining Eqs. (4) and (6), one obtains

$$\begin{bmatrix} \mathbf{M}_{rr} & \mathbf{M}_{rf} & \mathbf{C}_{\mathbf{q}_r}^T \\ \mathbf{M}_{fr} & \mathbf{M}_{ff} & \mathbf{C}_{\mathbf{q}_f}^T \\ \mathbf{C}_{\mathbf{q}_r} & \mathbf{C}_{\mathbf{q}_f} & \mathbf{0} \end{bmatrix} \begin{bmatrix} \ddot{\mathbf{q}}_r \\ \ddot{\mathbf{q}}_f \\ \boldsymbol{\lambda} \end{bmatrix} = \begin{bmatrix} (\mathbf{Q}_e)_r + (\mathbf{Q}_v)_f \\ (\mathbf{Q}_e)_f + (\mathbf{Q}_v)_f \\ \mathbf{Q}_c \end{bmatrix} . \tag{7}$$

This system of equations can be solved for the reference and elastic accelerations as well as for the vector of Lagrange multipliers. The accelerations can be integrated forward in time using a direct numerical integration method coupled with an iterative Newton-Raphson algorithm in order to check on the violation of the kinematic constraints. The numerical solution defines the generalized coordinates and velocities. On the other hand the vector of Lagrange multipliers $\boldsymbol{\lambda}$, can be used to calculate the generalized joint and driving constraint forces.

In our case the sprayer model is dynamically driven. A control model of the engine and transmission system is implemented in the computer model of the sprayer and used to drive the vehicle. This approach provides a more realistic model of the sprayer dynamics and in the earlier analysis was one of the critical elements in validation of the computer model with the real machine. The driving constraint forces implemented in the presented model were used to steer or maintain the driving direction of the vehicle. More details regarding modeling of the sprayer will be discussed later in the paper.

3. Computer model of the sprayer

The computer model of the sprayer consists of 22 bodies, which represent major components. They include cab, chassis, fuel tank, engine and pump set, chemical tank, ground, four wheels, four trailing links, four suspension arms, mast, two links connecting the boom with the mast, and the flexible boom. Each component is specified by its mass, moment of inertia, and location of center of gravity. Some of the components have variable mass. For example, a chemical tank capable of holding 1000 gallons of chemicals is almost 4000 kg heavier if it is fully filled. Similarly, the gasoline tank is almost 800 kg heavier when it is full. The fully loaded vehicle weighs about 15 ton. Figure 1 shows the location of these major components on the vehicle.

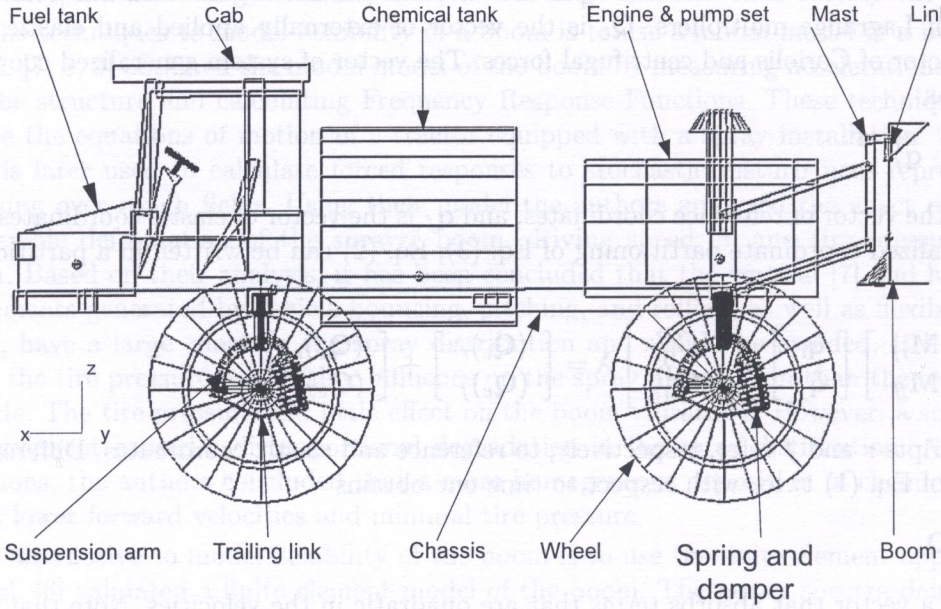

Fig. 1. Multibody model of the sprayer

Most of the components are connected to the chassis by bracket joints, which remove all relative six degrees of freedom. The bracket joints are placed at the components' center of gravity. However, other types of joints, force elements and constraints are used as connectors. For example, the cab is suspended on four isomounts. These isomounts are modeled using bushings that are six degrees of freedom force elements. The wheel suspension consists of suspension arm and trailing link. Suspension arms are connected to their respective trailing links by revolute joints at one end. At the other end, a coil spring with a damper connects these two elements as seen in Fig. 1. The mast is connected to the chassis by two revolute joints, distance constraint, and spring-damper that represents a hydraulic actuator used to raise and lower the boom. The orientation of the two revolute joints is in (y) direction of the coordinate system shown in Fig. 2.

The boom is connected to the mast by two links as seen in Fig. 2. Revolute joints are used at both ends of these links. So, the mast–link connection is modeled by a revolute joint, and the boom–link connection is modeled by a revolute joint. The orientation of these revolute joints is in (x) direction of the coordinate system shown in Fig. 2. From Fig. 2 it can be seen that the boom is connected to the mast at three points. The third connection is modeled by a difference constraint. This constraint keeps constant the longitudinal (x) component of the distance between the boom and the mast. The relative rotation of the boom with respect to the vehicle is controlled by two compressive springs, which connect the sides of the mast and the center of the boom as seen in Fig. 2. This system consisting of these two springs and the two links represents the boom suspension. Some of the vehicle natural frequencies are very close to the lowest natural frequencies of the flexible boom. For example, the 1.56 Hz vehicle pitching frequency is very close to the boom second natural frequency of 1.49 Hz.

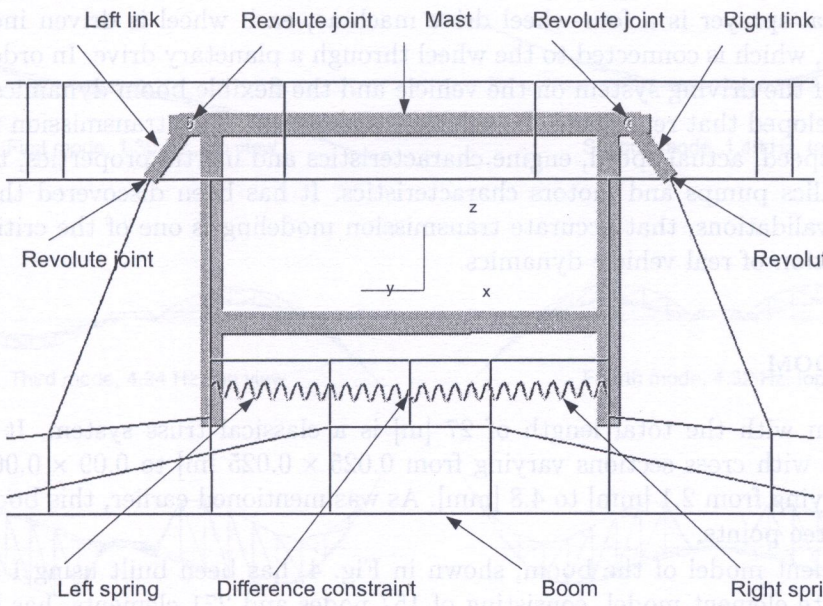

Fig. 2. Boom constraints

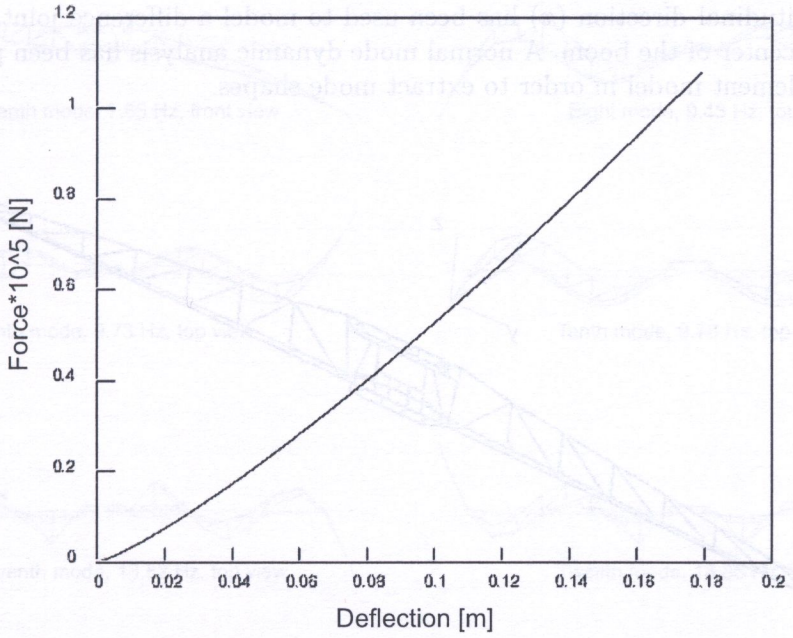

Fig. 3. Tire vertical stiffness

This may result in the coupling effect between the boom and the vehicle. As a matter of fact, subsequent studies show that the second mode seems to be dominant in defining the boom deflection.

All four wheels are connected to their respective trailing links by revolute joints in the computer model. The front suspension arms are connected to the chassis by revolute joints as well. These joints allow steering of the vehicle as desired. As mentioned earlier, the actual sprayer steering is performed by a set of kinematic constraints. Nonlinear characteristics of tires are implemented in the computer model in order to represent accurate dynamics of the real machine. These characteristics include tire stiffness and damping in vertical, longitudinal, and lateral direction. They also include cornering stiffness and rolling resistance. Figure 3 shows the implemented curve of the tire vertical force as a function of deflection.

Since the actual sprayer is a four-wheel drive machine, each wheel is driven independently by a hydraulic motor, which is connected to the wheel through a planetary drive. In order to accurately model the effect of the driving system on the vehicle and the flexible boom dynamics, a control system has been developed that represents the vehicle transmission. This transmission model includes: operator desired speed, actual speed, engine characteristics and inertia properties, transmission inertia, and hydraulics pumps and motors characteristics. It has been discovered through previous computer model validations, that accurate transmission modeling is one of the critical elements in proper representation of real vehicle dynamics.

4. Flexible boom

The sprayer boom with the total length of 27 [m] is a classical truss system. It is built out of rectangular tubes with cross sections varying from 0.025×0.025 [m] to 0.09×0.065 [m], and the wall thickness varying from 2.1 [mm] to 4.8 [mm]. As was mentioned earlier, this boom is connected to the mast at three points.

The finite element model of the boom, shown in Fig. 4, has been built using I-DEAS software package. This finite element model, consisting of 157 nodes and 271 elements, has been developed using beam elements. A set of constraints has been applied at nodes, which connect the boom with the mast of the sprayer. Revolute joint constraints allowing relative rotation between the boom and the mast have been used at connections between the boom and left and right links. A point constraint in longitudinal direction (x) has been used to model a difference joint, located between the mast and the center of the boom. A normal mode dynamic analysis has been performed on this constraint finite element model in order to extract mode shapes.

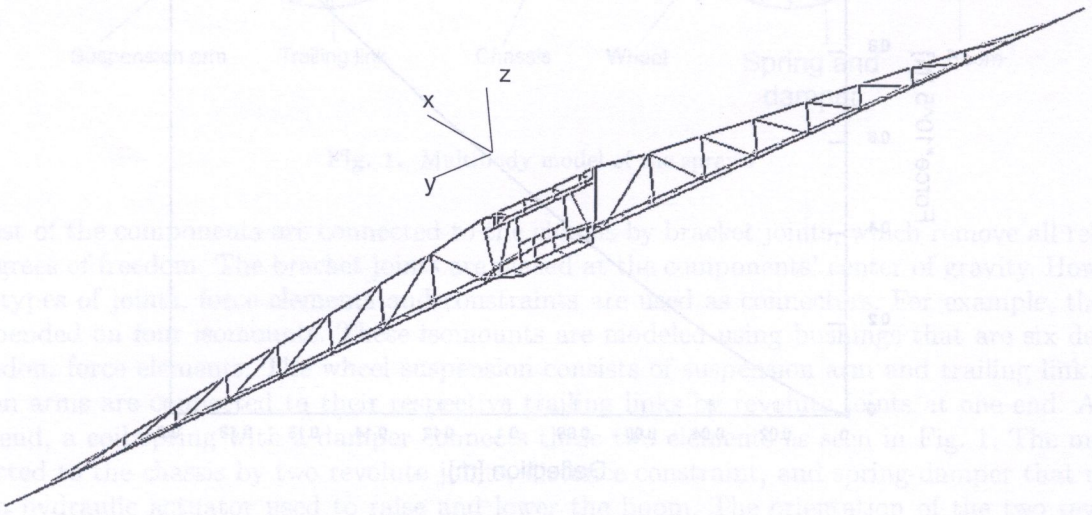

Fig. 4. Finite element model of the boom

A total of twelve normal mode shapes have been extracted from the finite element model and incorporated into the multibody model of the sprayer. Figure 5 shows mode shapes and natural frequencies of all twelve modes. As can be seen, the natural frequencies range from 1.30 Hz for the first mode to 13.88 for the twelfth mode. The first four modes represent almost pure fore-aft (longitudinal) bending of the boom. The fifth and sixth modes represent twisting of the boom. The seventh mode represents vertical bending. The eighth mode represents a combination of longitudinal bending and twisting. The ninth, tenth, eleventh, and twelve modes represent a combination of longitudinal and vertical bending as well as twisting. Figure 6 shows a vertical component of the complex modes.

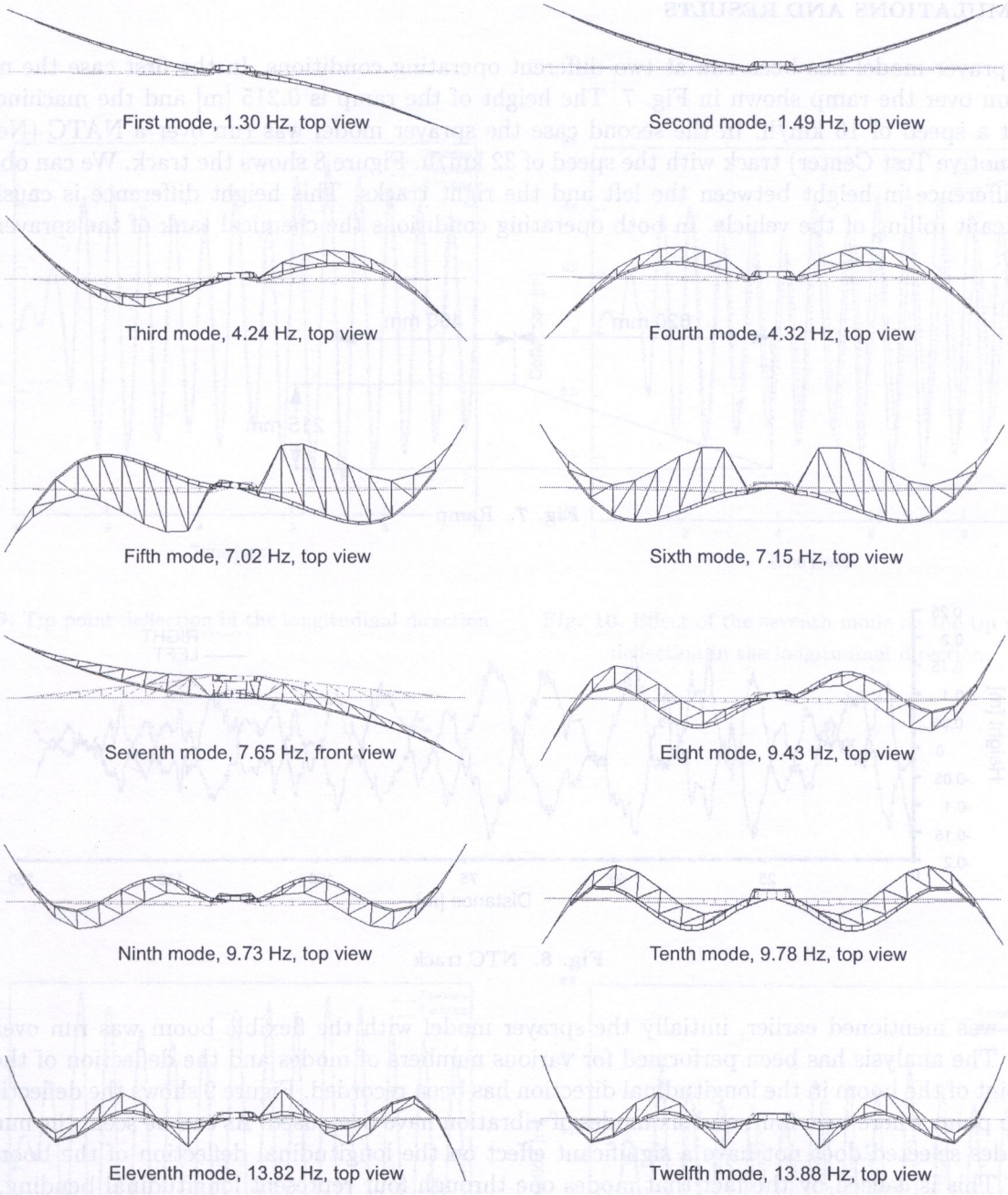

Fig. 5. Mode shapes

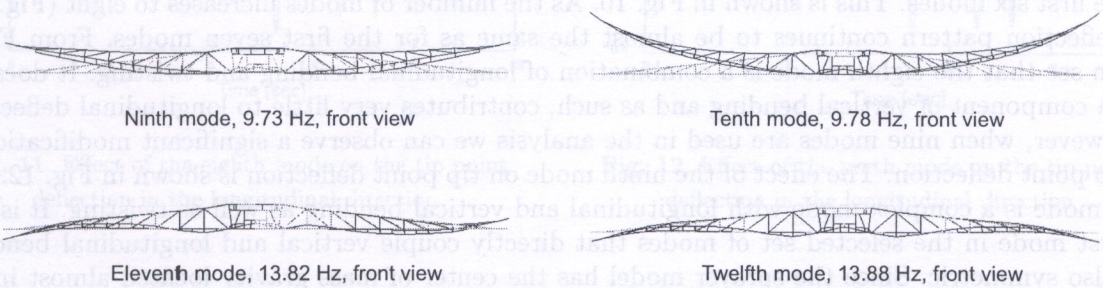

Fig. 6. Vertical component of deflection for higher modes

5. Simulations and results

The sprayer model has been run at two different operating conditions. In the first case the model was run over the ramp shown in Fig. 7. The height of the ramp is 0.215 [m] and the machine was run at a speed of 16 km/h. In the second case the sprayer model was run over a NATC (Nevada Automotive Test Center) track with the speed of 32 km/h. Figure 8 shows the track. We can observe the difference in height between the left and the right tracks. This height difference is causing a significant rolling of the vehicle. In both operating conditions the chemical tank of the sprayer was empty.

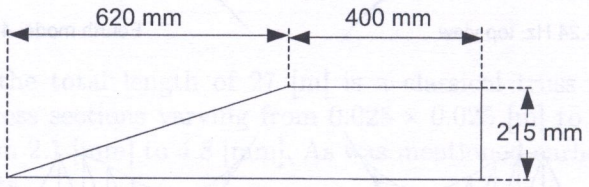

Fig. 7. Ramp

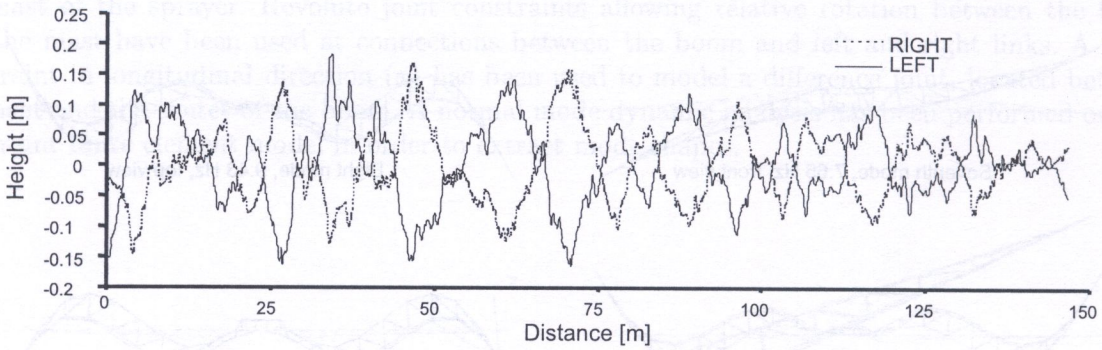

Fig. 8. NTC track

As was mentioned earlier, initially the sprayer model with the flexible boom was run over the ramp. The analysis has been performed for various numbers of modes and the deflection of the left tip point of the boom in the longitudinal direction has been recorded. Figure 9 shows the deflection of the tip point where two, four, and six modes of vibration have been used. As can be seen, the number of modes selected does not have a significant effect on the longitudinal deflection of the boom tip point. This is caused by the fact that modes one through four represent longitudinal bending, and the fifth and sixth modes represent twisting of the boom. None of these modes contribute to vertical deflection of the tip point. However, when the seventh mode is added into the set of selected modes to represent flexibility of the boom, the deflection of the tip point is then significantly different then for the first six modes. This is shown in Fig. 10. As the number of modes increases to eight (Fig. 11), the deflection pattern continues to be almost the same as for the first seven modes. From Fig. 5 we can see that the eighth mode is a combination of longitudinal bending and twisting. It does not have a component of vertical bending and as such, contributes very little to longitudinal deflection.

However, when nine modes are used in the analysis we can observe a significant modification in the tip point deflection. The effect of the ninth mode on tip point deflection is shown in Fig. 12. The ninth mode is a complex mode with longitudinal and vertical bending as well as twisting. It is also the first mode in the selected set of modes that directly couple vertical and longitudinal bending. It is also symmetric. Since the sprayer model has the center of mass gravity located almost in the geometrical center of the vehicle, and the model is uniformly driven by applying the same combined torque to the left and the right wheels, and the surface and the ramp are symmetric, it is more likely

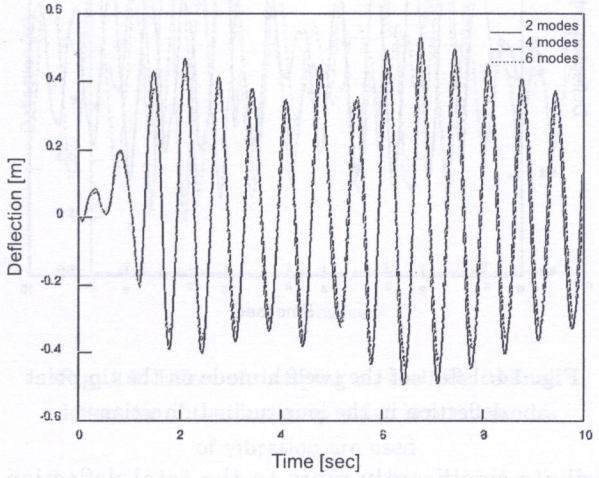

Fig. 9. Tip point deflection in the longitudinal direction

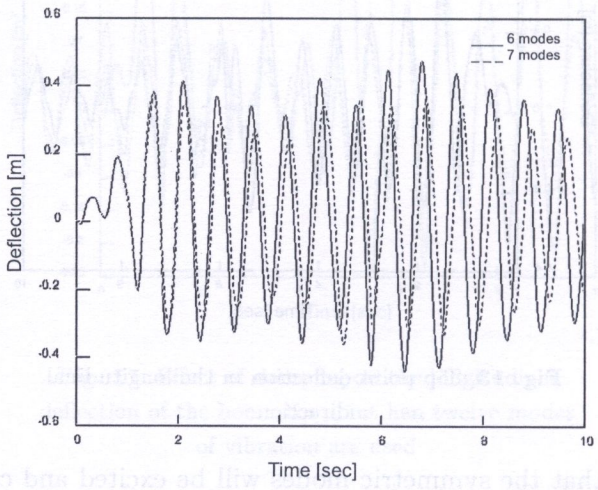

Fig. 10. Effect of the seventh mode on the tip point deflection in the longitudinal direction

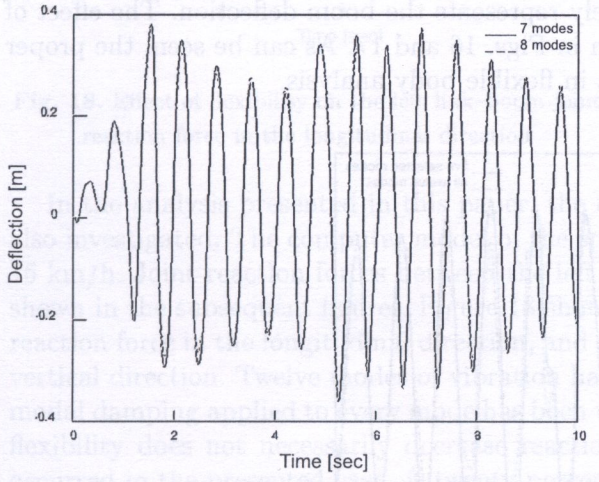

Fig. 11. Effect of the eighth mode on the tip point deflection in the longitudinal direction

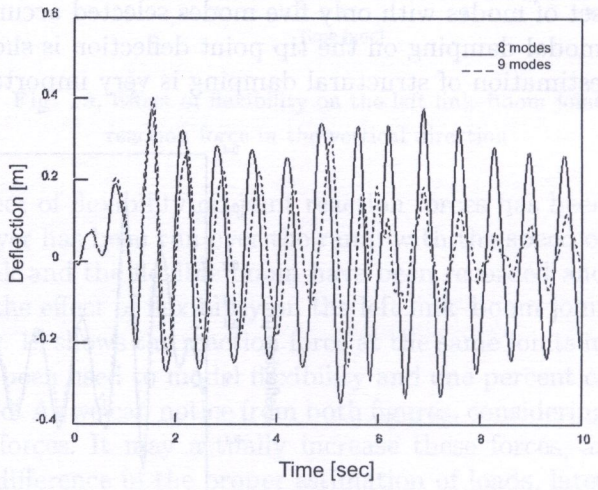

Fig. 12. Effect of the ninth mode on the tip point deflection in the longitudinal direction

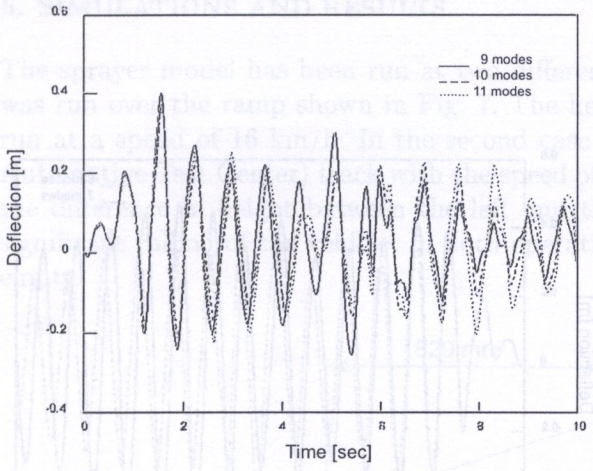

Fig. 13. Tip point deflection in the longitudinal direction

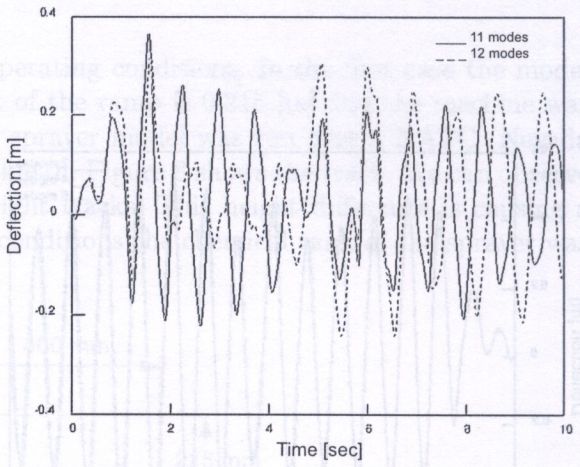

Fig. 14. Effect of the twelfth mode on the tip point deflection in the longitudinal direction

that the symmetric modes will be excited and contribute significantly more to the total deflection than asymmetric modes.

The contribution of the tenth and eleventh modes is shown in Fig. 13. Mode ten is symmetric and its effect on the overall deflection of the tip point is significantly larger then the eleventh mode. Figure 14 shows the tip point deflection when all twelve modes are used in the analysis. Since the twelfth mode represents a combination of longitudinal and vertical bending as well as twisting and the mode is symmetric, its contribution is very significant.

As it was pointed out earlier, the contribution of symmetric modes to represent the boom deflection during ramp crossing operation is overwhelming. Figure 15 shows the tip point deflection when two different sets of modes have been selected. The first set consists of only five modes of vibration and includes the second, seventh, ninth, tenth, and twelfth modes. All of the selected modes are symmetric except the seventh mode, which is asymmetric and represents vertical bending. The second set consists of all twelve modes used in the analysis. As can be noticed, the first set of modes with only five modes selected accurately represents the boom deflection. The effect of modal damping on the tip point deflection is shown in Figs. 16 and 17. As can be seen, the proper estimation of structural damping is very important in flexible body analysis.

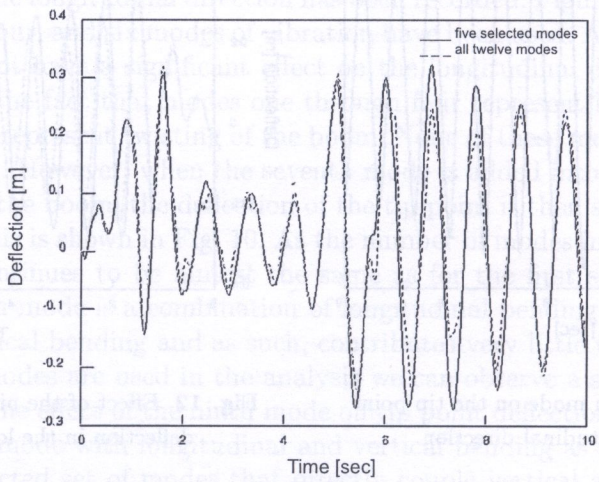

Fig. 15. Contribution of symmetric modes to the deflection of the boom tip point in the longitudinal direction

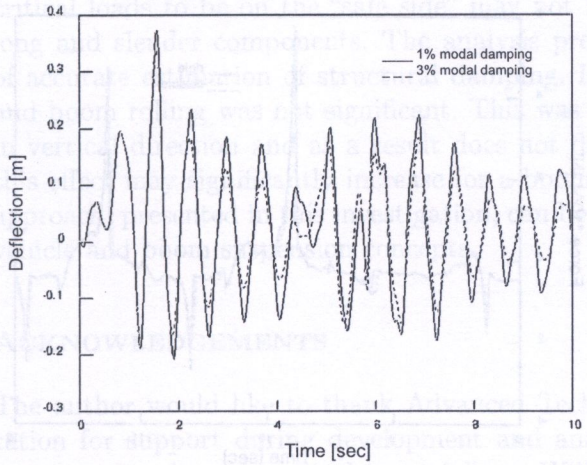

Fig. 16. Effect of damping on the longitudinal deflection of the boom tip point hen ten modes of vibration are used

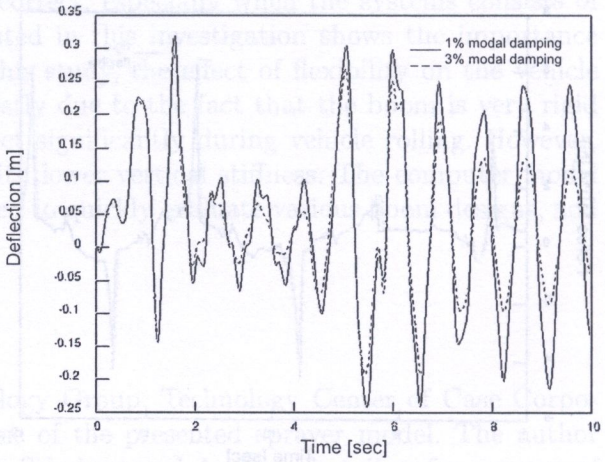

Fig. 17. Effect of damping on the longitudinal deflection of the boom tip point hen twelve modes of vibration are used

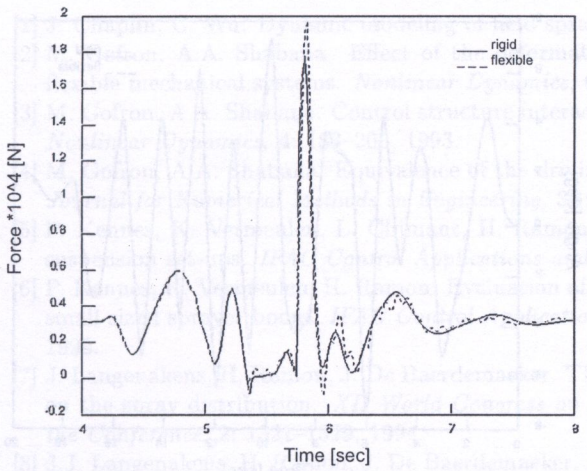

Fig. 18. Effect of flexibility on the left link–boom joint reaction force in the longitudinal direction

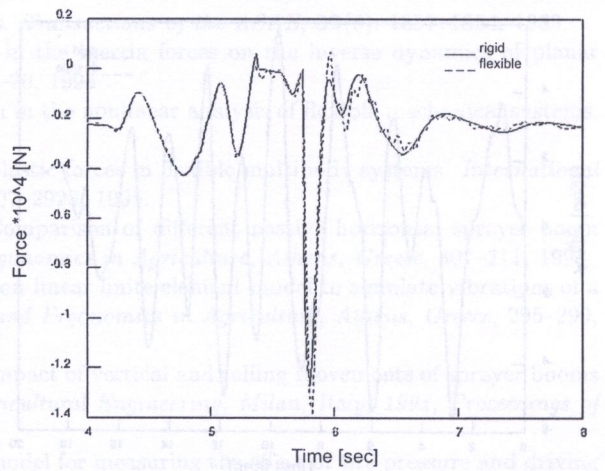

Fig. 19. Effect of flexibility on the left link–boom joint reaction force in the vertical direction

In the analysis presented in this paper, the effect of flexibility on joint reaction forces has been also investigated. The computer model of the sprayer has been run over the ramp with the speed of 16 km/h. Joint reaction forces between the left link and the flexible boom have been recorded and shown in the subsequent figures. Figure 18 shows the effect of flexibility on the left link–boom joint reaction force in the longitudinal direction, and Fig. 19 shows the reaction force at the same joints in vertical direction. Twelve modes of vibration have been used to model flexibility and one percent of modal damping applied to every mode has been used. As we can notice from both figures, considering flexibility does not necessarily decrease reaction forces. It may actually increase these forces, as occurred in the presented case. A twenty percent difference in the proper estimation of loads, later used for the machine design, can have a significant impact on the life and safety of the design.

Figures 20–23 show several results for a simulation considering a speed of 32 km/h over an NATC track. As we can see from Fig. 8, the track is very rough with large profile differences between the left and the right tracks. These differences in the tracks height exceeding 0.3 [m] cause significant vehicle rolling. Figures 20 and 21 show the effect of flexibility on left link–boom reaction forces in longitudinal and vertical directions respectively. As in the ramp case, when sprayer runs over the NATC track, the flexibility generally increased reaction forces.

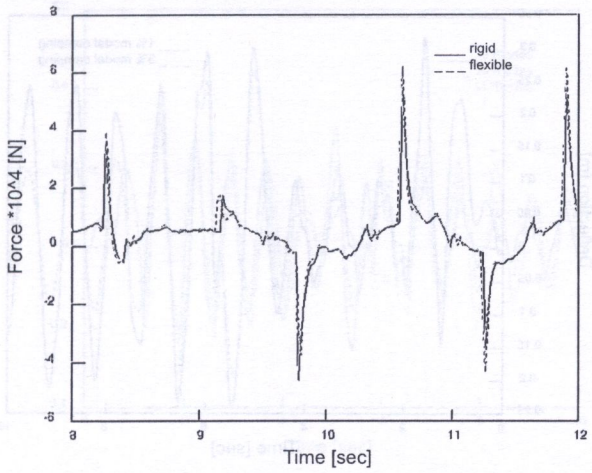

Fig. 20. Effect of flexibility on the reaction force (left link–boom joint, longitudinal reaction force, NATC track)

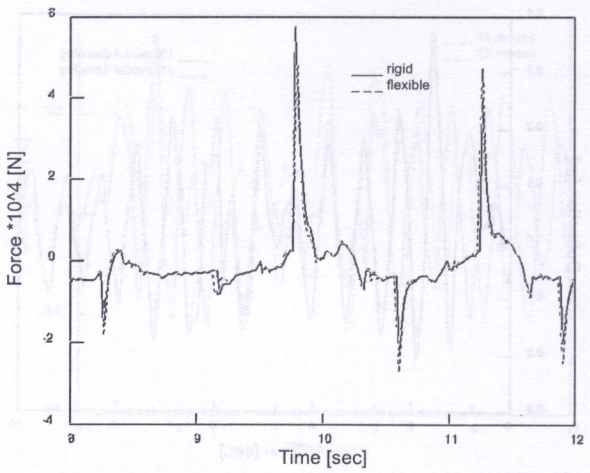

Fig. 21. Effect of flexibility on the reaction force (left link–boom joint, vertical reaction force, NATC track)

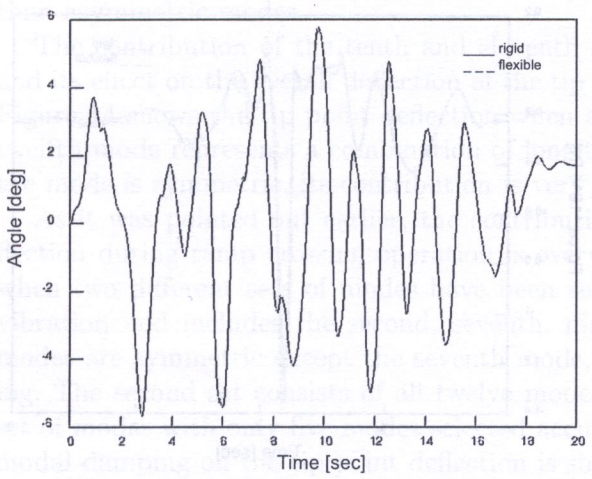

Fig. 22. Effect of flexibility on sprayer rolling

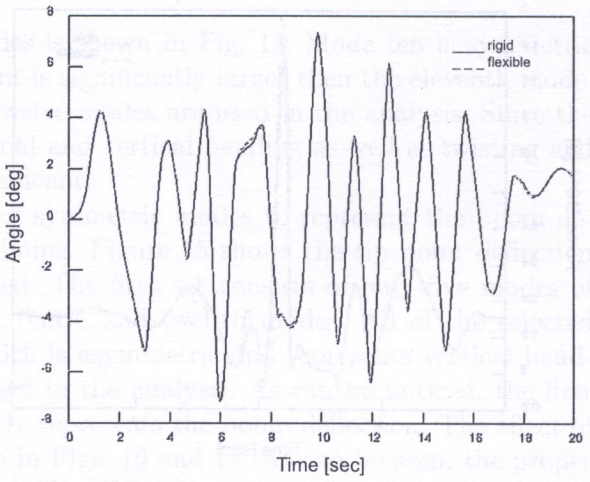

Fig. 23. Effect of flexibility on boom rolling

Finally, one of the critical interests in the designing of a sprayer is to calculate the vehicle rolling and the effect of flexibility on the vehicle rolling when the machine is subjected to extreme operating conditions. Figures 22 and 23 show respectively vehicle and boom rolling when the boom is modeled as rigid and flexible. As it can be seen the effect of flexibility on vehicle and boom rolling is minimal. This effect is minimal mostly due to high stiffness of the boom in vertical direction.

6. Conclusions

In this study, a finite element model of the boom has been developed and used to obtain modal characteristics of the structure. These characteristics have been incorporated into a multibody model of the sprayer, which was validated with the real vehicle in earlier studies. The effect of the number of modes, the effect of structural damping on boom deformation, and the effect of flexibility on boom reaction forces and vehicle and boom rolling has been analyzed in this investigation. It has been shown that proper selection of modes is critical in accurate representation of boom flexibility.

It was also shown that flexible bodies with significant deflections could generate larger loads than those modeled as rigid. Thus, the assumption that modeling systems with rigid bodies ensures

critical loads to be on the "safe side" may not be correct, especially when the systems consists of long and slender components. The analysis presented in this investigation shows the importance of accurate estimation of structural damping. In this study, the effect of flexibility on the vehicle and boom rolling was not significant. This was mostly due to the fact that the boom is very rigid in vertical direction and as a result does not deflect significantly during vehicle rolling. However, this effect may significantly increase for a boom with lower vertical stiffness. The computer model approach, presented in this investigation, can be used to quickly evaluate various boom designs, and vehicle and boom suspension concepts.

Acknowledgements

The author would like to thank Advanced Technology Group, Technology Center of Case Corporation for support during development and analysis of the presented sprayer model. The author expresses his sincere gratitude especially to William Schubert and Andrey Skotnikov for support of this publication.

References

[1] J. Chaplin, C. Wu. Dynamic modeling of field sprayers. *Transactions of the ASAE*, **32**(6): 1857–1864, 1989.

[2] M. Gofron, A.A. Shabana. Effect of the deformation in the inertia forces on the inverse dynamics of planar flexible mechanical systems. *Nonlinear Dynamics*, **6**: 1–20, 1994.

[3] M. Gofron, A.A. Shabana. Control structure interaction in the nonlinear analysis of flexible mechanical systems. *Nonlinear Dynamics*, 4: 183–206, 1993.

[4] M. Gofron, A.A. Shabana. Equivalence of the driving elastic forces in flexible multibody systems. *International Journal for Numerical Methods in Engineering*, **38**: 2907–2928, 1995.

[5] P. Kennes, K. Vermeulen, L. Clijmans, H. Ramon. Comparison of different passive horizontal sprayer boom suspension set-ups. *IFAC Control Applications and Ergonomics in Agriculture, Athens, Greece*, 307–311, 1998.

[6] P. Kennes, K. Vermeulen, H. Ramon. Evaluation of a non-linear finite element model to simulate vibrations of a small sized sprayer boom. *IFAC Control Applications and Ergonomics in Agriculture, Athens, Greece*, 295–299, 1998.

[7] J. Langenakens, H. Ramon, J. De Baerdemaeker. The impact of vertical and rolling movements of sprayer booms on the spray distribution. *XII World Congress on Agricultural Engineering, Milan, Italy, 1994, Proceedings of the Conference*, **2**: 1321–1329, 1994.

[8] J.J. Langenakens, H. Ramon, J. De Baerdemaeker. A model for measuring the effect of tire pressure and driving speed on horizontal sprayer boom movements and spray pattern. *Transactions of ASAE* **38**: 65–72, 1995.

[9] J.J. Langenakens, H. Ramon, J. De Baerdemaeker. The effect of boom movements on spray distribution, enabling technologies for land use and resource management. *Proceedings 5th International Congress for Computer Techology in Agriculture, June 29–July 5, 1994, Stoneleigh Park, Warwickshire, UK*, **11**: 93–96, 1994.

[10] Y. Lardoux, C. Sinfort, A. Miralles, B. Bonicelli, F. Sevila. Dynamic effect of boom movements on spray distribution. *Proceeding of ASAE Annual International Meeting, Orlando, Florida*, 1998.

[11] H.S. Nielsen, P.H. Sorensen. Active suspension for a field sprayer boom. *IFAC Control Applications and Ergonomics in Agriculture, Athens, Greece*, 277–282, 1998.

[12] C. Sinfort, Y. Lardoux, A. Miralles, P. Enfalt, K. Alness, S. Andersson. Comparison between measurements and predictions of sprayer pattern from a moving boom sprayer. *Aspects of Applied Biology*, **48**: 1–8, 1997.